Creep and Ductility in an Al-Cu Solid-Solution Alloy

PRABIR K. CHAUDHURY and FARGHALLI A. MOHAMED

High-temperature creep was investigated in an Al-3 wt pct Cu alloy at temperatures in the range of 773 to 853 K and at a normalized shear stress range extending from 10^{-5} to 7×10^{-4}. The results show the presence of three distinct regions. In region I (low stresses), the stress exponent is 4.5 and the activation energy is 155 kJ/mole. In region II (intermediate stresses), the stress exponent is 3.2 and the activation energy is 151 kJ/mole. In region III (high stresses), the stress exponent is 4.5 and the activation energy is 205 kJ/mole. Creep curves obtained in the three regions exhibit a normal primary stage, but the extent of the stage is less pronounced in region II than in regions I and III. The creep characteristics in regions I and II, along with the values of the transition stresses between the two regions, are in conformity with the prediction of the deformation criterion for solid-solution alloys. While the advent of region III (high stresses) correlates well with dislocation breakaway from a solute-atom atmosphere, the creep characteristics in this region are not entirely consistent with any of the existing high-stress creep mechanisms. The plot of elongation to fracture *vs* initial strain rate at 853 K exhibits two peaks at strain rates of 1×10^{-4} and 6×10^{-4} s^{-1}. The first peak (1×10^{-4} s^{-1}) is attributed to the variation of the stress exponent for creep in the alloy with strain rate, and the second peak (6×10^{-4} s^{-1}) appears to reflect the effect of solute drag on dislocation velocity.

I. INTRODUCTION

In creep analysis, the stress dependence of creep rate is generally deduced from plotting the steady-state creep rate as a function of the applied stress and applying the relation:

$$n = \left.\frac{\partial \ln \dot{\gamma}}{\partial \ln \tau}\right|_T \qquad [1]$$

where n is the stress exponent measured at constant temperature, T, $\dot{\gamma}$ is the steady-state shear creep rate, and τ is the applied shear stress.

Earlier creep experiments[1-4] revealed the presence of two limiting values of the stress exponent, n, in solid-solution alloys. The upper limiting value is close to 5 and is observed in alloys whose creep behavior, like that of pure metals, exhibits the characteristics of climb control:[1,2,3] extensive primary creep, subgrain formation, and dependence of the creep rate on the stacking fault energy of the alloy. The lower limiting value is 3 and is noted in alloys whose creep behavior exhibits the characteristics of viscous glide control:[1,2,3] brief primary creep, random distribution of dislocations, and apparent insensitivity of the creep rate to changes in stacking fault energy.

It was suggested[2-5] that the creep behavior of a solid-solution alloy may be controlled by the sequential processes of dislocation climb and viscous glide. On the basis of this suggestion, it was predicted[2,3,5] that under a favorable combination of material parameters (such as the atom misfit ratio) and experimental variables (such as stress), the creep behavior of an alloy would exhibit a transition from climb-controlled behavior at low stresses to viscous glide-controlled behavior at intermediate stresses.

Several sets of experimental results[5-10] that support the predicted transition from dislocation climb to viscous glide, with increasing stress, are now available. These include (a) a change in the stress exponent for creep in Al-Mg alloys[6,9-11] and an Al-21 wt pct Zn alloy[12] from a value of 4.5 at low stresses to a value of about 3 at intermediate stresses; this change in stress exponent is in agreement with the mechanical aspect of the prediction; and (b) a corresponding change in the creep substructure of two Al-Mg alloys[9,10] from that typical of dislocation climb (significant tendency to form well-developed subgrains) to that typical of viscous glide (random distribution of dislocations) with increasing stress; this finding is in accordance with the substructural aspect of the prediction.

In addition to providing evidence in support of the predicted transition from dislocation climb to viscous glide, the experimental data on Al-Mg alloys[11] and an Al-21 wt pct Zn alloy [12] revealed the presence of another transition at high stresses. This transition is manifested by a change in stress exponent from about 3 (viscous glide) to higher values and has been attributed to dislocation breakaway from a solute-atom atmosphere.

The observation that at constant temperature, the stress exponent, n, for creep in a solid-solution alloy changes from a value of 5 at low stresses to a value of 3 at intermediate stresses and then increases again at high stresses leads to the following expectation: the ductility data of the alloy, when plotted as the elongation to fracture *vs* stress or strain rate, would exhibit a maximum at intermediate stresses or strain rates. This expectation is based on the results of several recent analyses[13-17] which demonstrate that ductility, defined as the percentage elongation to fracture, is a sensitive function of the stress exponent; in general, the lower the stress exponent, the higher the ductility of the material. A very recent investigation[18] on Al-21 wt pct Zn has shown the presence of maximum ductility at intermediate strain rates in agreement with the above expectation.

The purpose of this paper is two-fold: (a) to report the data of a detailed investigation conducted, over wide ranges of experimental conditions, on the creep behavior and ductility of an Al-3 wt pct Cu (Al-1.3 at. pct Cu) solid-solution alloy; and (b) to examine these data in the light of recent advances made in rationalizing the creep behavior of solid-solution alloys.

PRABIR K. CHAUDHURY, a Graduate Research Assistant, and FARGHALLI A. MOHAMED, Professor, are with the Department of Mechanical Engineering, University of California-Irvine, Irvine, CA 92717.

Manuscript submitted January 26, 1987.

II. EXPERIMENTAL TECHNIQUES

Al-3 wt pct Cu (equivalent to 1.3 at. pct Cu) was supplied by Kaiser Aluminum and Chemical Corporation. The alloy was prepared from aluminum of 99.99 pct purity and copper of 99.99 pct purity. The final material contained the following elements in weight percent: 2.97Cu, 0.007Si, 0.003Fe, 0.001Mg, 0.003Zn, <0.001Mn, <0.001Ti, and the remainder is aluminum.

Double-shear and tensile specimens of shape and dimensions described elsewhere[5,19-21] were machined from the material. Prior to testing, all specimens were annealed *in situ* for 15 hours at 855 K for the dual purpose of removing the effects of machining and producing a stable, uniform grain size. The grain size was measured using a procedure that is based on deformation by grain boundary sliding and that was adopted very recently in the case of Al-Zn alloys;[12,22] the phase transformation which occurred as specimens were cooled made it difficult to adopt standard metallographic techniques applied successfully in the case of Al-Mg alloys.[10,11] This procedure, when repeated, resulted in a consistent grain size of 3 mm.

Double-shear experiments were performed either on a suitably designed creep-testing machine at constant load or on an Instron machine operating at a constant rate of crosshead displacement; for the present specimen configuration, constant load implies constant stress and constant crosshead displacement is equivalent to constant strain rate. The procedures of monitoring test temperature and measuring creep strain are the same as those described in detail elsewhere.[6,8,9,11,12]

On the creep machine, steady-state creep rates were measured over a range of stresses from 0.2 MPa to 8 MPa. On the Instron machine, steady-state stresses were determined over a range of strain rates extending from 2×10^{-4} s^{-1} to 10^{-1} s^{-1}. These ranges of stresses (creep) and strain rates (Instron) were scanned at three different temperatures, 853 K, 813 K, and 778 K, which fall in the solid-solution range; the solid-solution range for Al-3 pct Cu is narrow and extends from 740 to 865 K. The use of more than one testing temperature in the present investigation serves two purposes: (a) to determine the activation energy for creep, and (b) to examine transitions in the creep behavior of the alloy, if present, as a function of temperature.

In order to check the values of the activation energy at both low and intermediate stresses, where strain rates are reasonably slow ($\dot{\gamma} < 10^{-4}$ s^{-1}), the procedure of temperature cycling[23] was adopted during creep. In this procedure, a specimen was subjected to a number of rapid changes, during creep, of the order of 15 K while under constant stress. The activation energy was then calculated after each temperature change from the relation:

$$Q = \frac{R \ln(\dot{\gamma}_2 G_2^{n-1} T_2 / \dot{\gamma}_1 G_1^{n-1} T_1)}{(T_2 - T_1)/T_1 T_2} \qquad [2]$$

where $\dot{\gamma}_1$ and $\dot{\gamma}_2$ are the instantaneous creep rates immediately before and after the change in temperature from T_1 to T_2, and G_1 and G_2 are the corresponding shear moduli. In the absence of information on the variation of the shear modulus of Al-3 pct Cu, with temperature in the solid-solution range, the equation describing the relation between G and T for aluminum was used.

Ductility tests were performed at a constant temperature of 853 K. Each tensile specimen was pulled in tension at a single rate of cross-head displacement on the Instron testing machine. The strain rates quoted therefore refer to initial strain rates calculated from the initial gage length. Also, ductility tests were conducted on pure aluminum (99.99 pct) under similar experimental conditions (homologous temperature and grain size) to provide a comparison between the behavior of Al-3 pct Cu and that of the metal.

III. EXPERIMENTAL RESULTS

A. *Stress Dependence of the Steady-State Strain Rate*

The dependence of strain rate on stress, under steady-state conditions, was investigated by conducting a series of double-shear tests at a constant temperature on the creep machine and the Instron machine, and by plotting shear strain rate, $\dot{\gamma}$, as a function of shear stress, τ, on a logarithmic scale. Figure 1 depicts this form of plot for three different temperatures, 853 K, 813 K, and 773 K. Examination of the data of this figure reveals several findings. First, there are three regions of deformation: low-stress region (region I), intermediate-stress region (region II), and high-stress region (region III). The values of the stress exponent, n, in regions I, II, and III are 4.5, 3.2, and 4.5, respectively. Second, region II (the intermediate-stress region) which exhibits a stress exponent of about 3.2 covers an increasing range of measurable shear strain rate with decreasing temperature: at $T = 853$ K, region II covers two

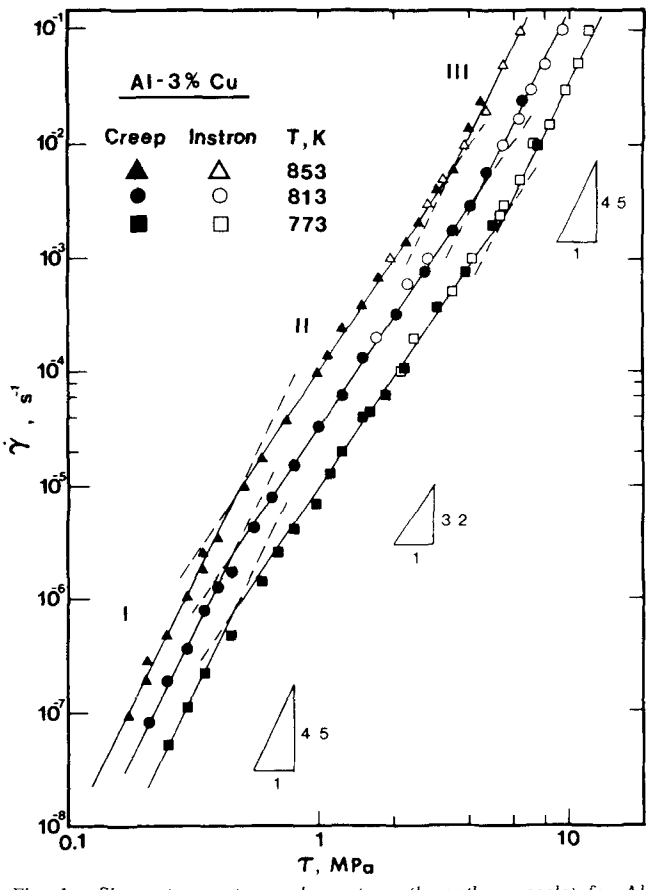

Fig. 1—Shear strain rate *vs* shear stress (logarithmic scale) for Al-3 wt pct Cu at various temperatures from 773 to 853 K

and a half orders of magnitude of strain rate whereas at $T = 773$ K, it extends over three orders of magnitude of strain rate. Third, while there is a slight decrease in the value of the normalized transition shear stress between region I (low-stress region) and region II (intermediate-stress region) with decreasing temperature, the opposite is true for the case of the normalized transition stress between region II and region III (high-stress region); with decreasing temperature from 853 K to 773 K, $(\tau/G)_{\text{I-II}}$ decreases from 3×10^{-5} to 2.7×10^{-5} whereas $(\tau/G)_{\text{II-III}}$ increases from 2.1×10^{-4} to 3.1×10^{-4}. Finally, there is excellent agreement between experimental data of creep (applying external stresses and measuring steady-state creep rates) and those of Instron (imposing strain rates and measuring the steady-state stresses) in regions II and III.

B. *Creep Curves*

Typical examples of creep curves obtained in regions I, II, and III are presented in Figure 2. Examination of these creep curves, and others, indicates the presence of two main features: (a) a normal primary stage ($d\dot{\gamma}/dt < 0$) exists in all creep curves of the three regions before steady-state creep is reached, and (b) the extent of the primary stage is more pronounced in regions I ($n \simeq 4.5$) and III ($n = 4.5$) than in region II ($n = 3.2$).

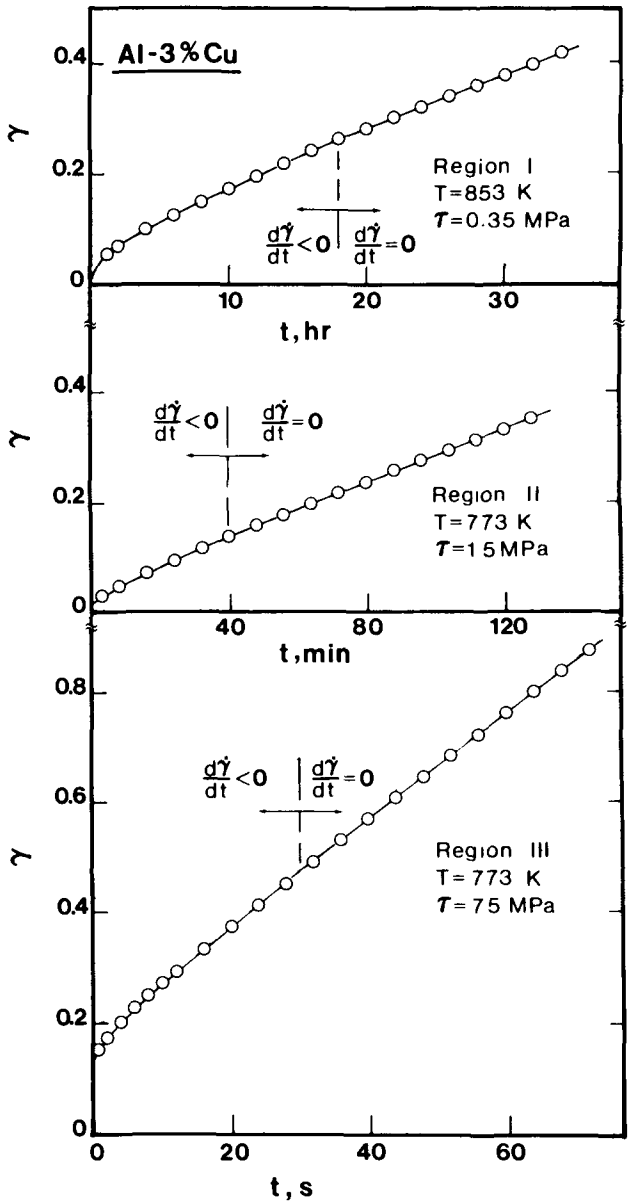

Fig. 2—Typical plots of shear strain *vs* time (creep curves) for regions I, II, and III.

C. *Activation Energy for Creep*

Figure 3 provides two examples for the application of the temperature cycling procedure in regions I and II. The results of the temperature cycling procedure, when combined with the creep data of Figure 1 and plotted in the form of logarithmic $\dot{\gamma}G^{n-1}T$ (where $n = 3.2$ for region II and $n = 4.5$ for region I) as a function of $1/T$ using stress levels of 0.3 MPa and 1.5 MPa for regions I and II, respectively, yielded, as shown by Figure 4, two nearly parallel straight lines. This indicates that the activation energies associated with regions I and II are nearly equal; a least square analysis of the data of Figure 4 gave activation energies of 155 ± 5 kJ/mole and 151 ± 6 kJ/mole for regions I and II, respectively.

It was not possible to use the temperature cycling procedure in region III (high-stress region), basically because the creep rates associated with this region are fast. In this case, the activation energy was determined from the creep data of Figure 1 as 205 kJ/mole. This value of the activation energy for creep in region III is considerably higher than

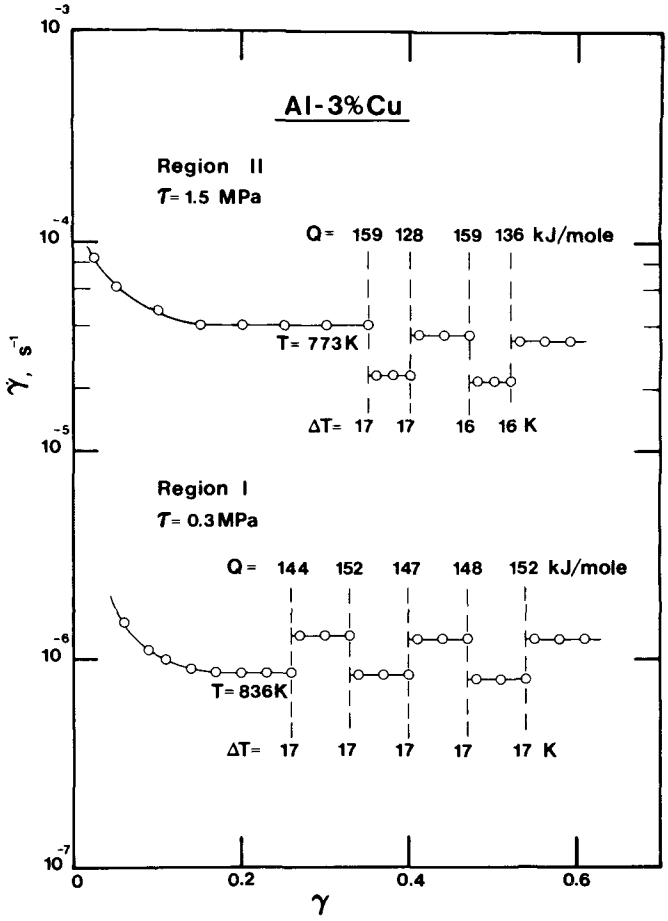

Fig. 3—Shear strain rate *vs* shear strain, showing the determination of the activation energy for creep in regions I and II from the temperature cycling procedure.

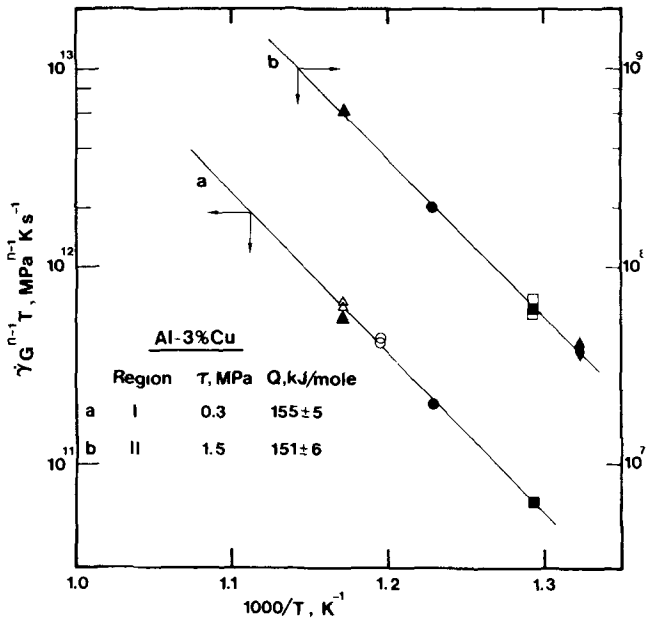

Fig. 4—Determination of the activation energy for creep in regions I and II by plotting log ($\dot{\gamma}G^{n-1}T$) *vs* $1/T$. Experimental data were taken from Figs. 1 and 3.

those of the activation energies in regions I and II (low and intermediate stress regions).

D. *Ductility*

Results of ductility tests at the highest stress of creep testing for Al-3 pct Cu are given in Figure 5, in which the percentage elongation to fracture, e_f pct ($e = \Delta L/L_0$, where ΔL is the increase in length and L_0 is the initial length of the specimen), is plotted as a function of initial tensile strain rate, $\dot{\varepsilon}$. Also included in the figure are the ductility data for pure aluminum, which were obtained under the same experimental conditions of homologous temperature ($T \simeq 0.99\ T_m$, where T_m is the melting temperature) and grain size.

For Al-3 pct Cu, e_f pct increases from $\simeq$ 300 at 10^{-5} s^{-1} to a maximum of 355 at 10^{-4} s^{-1}, exhibits a minimum of 230 at 3×10^{-4} s^{-1}, rapidly increases to 285 at 6×10^{-4} s^{-1}, and finally decreases slowly and continuously to 155 at 10^{0} s^{-1}. By contrast, the value of e_f for Al remains essentially constant ($\simeq$ 150) over the whole range of strain rates except the very high strain rates (10^{-1} and 10^{0} s^{-1}) where a slight decrease in ductility occurs.

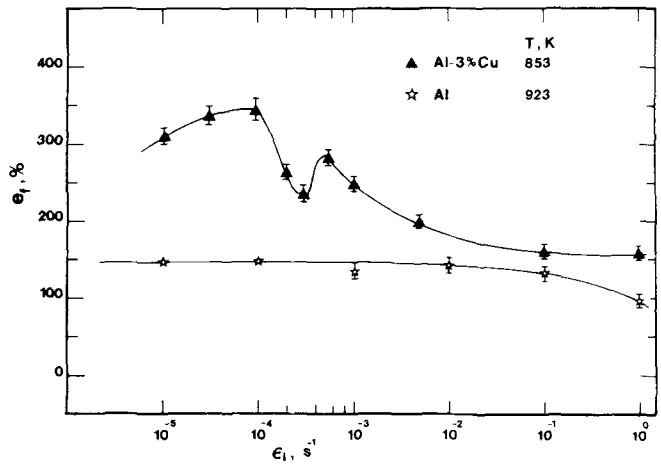

Fig. 5—Strain to failure (elongation pct) *vs* initial strain rate for Al-3 wt pct Cu at 853 K and Al at 923 K.

Examination of the tensile specimens after fracture reveals two findings: (a) failure occurs by necking over the whole range of strain rates, and (b) no significant cavitation, even in the vicinity of the fracture tip of the specimen, is present; in a few cases, a very small number of randomly distributed cavities were seen within the gage length at points remote from the fracture tip.

IV. DISCUSSION

It was shown that under conditions of steady-state deformation, the dependence of the normalized creep rate on the normalized applied stress at large grain sizes may be represented by an expression of the form:[2,24]

$$\frac{\dot{\gamma}kT}{DGb} = A(\tau/G)^n \qquad [3a]$$

with

$$D = D_0 \exp -Q/RT \qquad [3b]$$

where $\dot{\gamma}$ is the shear creep rate, k is Boltzmann's constant, T is the absolute temperature, D is the diffusion coefficient that characterizes the creep process, G is the shear modulus, b is the Burgers vector, A is a dimensionless constant, τ is the applied shear stress, n is the stress exponent, Q is the activation energy for the diffusion process that controls the creep behavior, and D_0 is the frequency factor.

Although the creep behavior of a polycrystalline material may, in general, be ascribable to a number of different processes, a single deformation process may, under favorable experimental conditions, be responsible for the measured creep rate, resulting in the presence of a distinct deformation region whose characteristics reflect the details of such a process. On this basis, the rate-controlling process for a well-defined deformation region may be identified by comparing experimental results obtained in the region with those predicted for various basic processes.

The present experimental results show the presence of three regions of deformation, and it is appropriate to examine separately the data of each region in the light of creep characteristics established for basic deformation processes in solid-solution alloys.

A. *Region I (Low-Stress Region)*

In this region, the stress exponent of 4.5, which is essentially equal to that reported for pure Al, along with the presence of extensive primary creep, is suggestive of the dominance of some form of dislocation climb process.[1-3,25] In addition, although there are no well-documented data on diffusion of Al in Al-3 pct Cu, the experimental activation energy of 155 kJ/mole is very close to that reported for self-diffusion in Al[19] ($\simeq$ 143.4 kJ/mole).

The creep behavior of Al-3 pct Cu in the low-stress region is similar in trend to that reported for Al-Mg alloys[6,9,10] and Al-21 wt pct Zn[12] under comparable experimental conditions (homologous temperature, normalized stresses, and grain size). Earlier analyses, published elsewhere,[6,9-12] of the mechanical data on Al-Mg alloys and the Al-

21 wt pct Zn solid-solution alloy have led to the conclusion that the creep behavior of these alloys at low stresses is also controlled by some form of dislocation climb process. More importantly, an examination of dislocation substructure* in two Al-Mg alloys[9,10] following creep at low stresses, where a stress exponent of 4.5 was measured, revealed the presence of well-developed subgrains, a substructural feature which is observed in metals whenever dislocation climb is the rate-controlling process.

*Because of the phase transformation occurring in Al-3 pct Cu upon cooling from test temperature under load, reliable microstructural data for the alloy cannot be obtained.

In Figure 6, the creep data obtained in region I at various stresses and different temperatures (Figure 1) were normalized in terms of Eq. [3] by plotting ($\dot{\gamma}kT/DGb$) against τ/G on a logarithmic scale; D_0, Q, and b were taken as 1.86 cm^2/s,[19] 155 kJ/mole, and 2.86×10^{-8} cm, respectively. For the purpose of comparison, Al data obtained in previous investigations[26,27] under a similar normalized temperature range were also included in Figure 6 and are represented by a broken line. As seen in the figure, the normalized creep data of Al-3 pct Cu fit a single straight line which falls very close to the line representing Al, suggesting that the stacking fault energy of the alloy, Γ, may be nearly equal to that for Al[28] (Γ_{Al} = 200 mJ/m^2). This suggestion is based on the finding of an analysis[29] of the creep

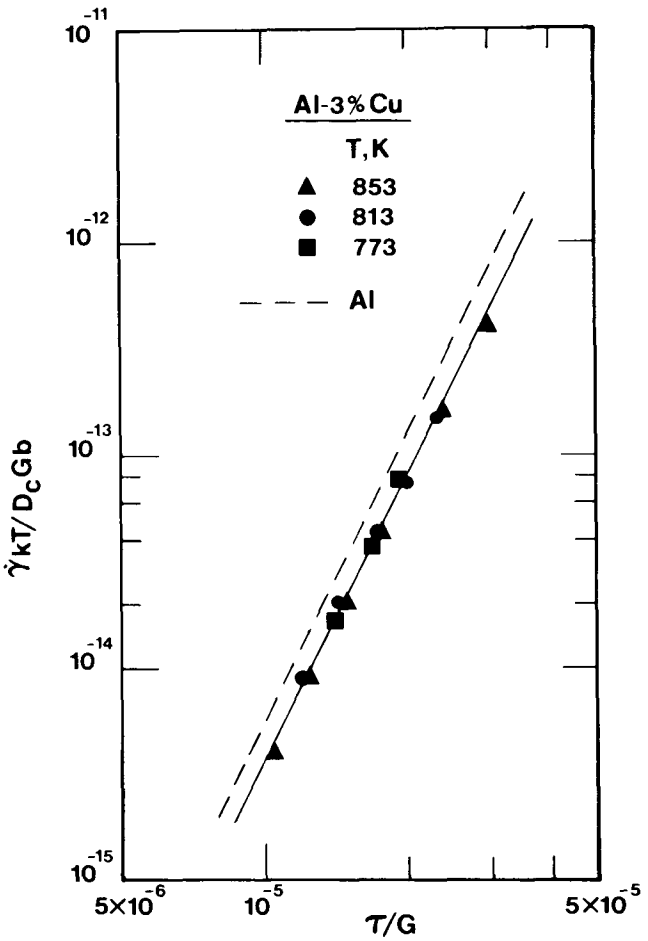

Fig. 6—Normalized creep rate *vs* normalized shear stress (logarithmic scale) for Al-3 wt pct Cu in region I. Normalized creep data of pure Al are included.[26,27]

data of various fcc metals and solid-solution alloys which shows that under the condition of climb control, the normalized creep rate, $\dot{\gamma}_N (= \dot{\gamma}kT/DGb)$, is related to $(\Gamma/Gb)^3$; this cubic dependence of the normalized creep rate on the normalized stacking fault energy was most recently rationalized[30,31] in terms of two relations: (a) a second power dependence of the climb velocity on Γ/Gb, and (b) a linear power dependence of the mobile dislocation density on Γ/Gb. The stacking fault energy of Al-3 pct Cu inferred from Figure 6, by using the relation: $(\dot{\gamma}_N)Al/(\dot{\gamma}_N)$ alloy $\simeq (\Gamma_{Al}/\Gamma_{alloy})^3$, is 180 mJ/m^2, a value which is comparable to those estimated for other dilute Al alloys, including Al-1 pct Mg[32] (190 mJ/m^2) and Al-2 at. pct Zn[33] (200 mJ/m^2).

B. *Region II (Intermediate-Stress Region)*

In this region, which prevails at intermediate stresses, viscous-glide creep[34] appears to account for the deformation characteristics of Al-3 pct Cu which include: (a) a stress exponent of 3.2, (b) a brief primary creep, and (c) an activation energy for creep ($\simeq$ 151 kJ/mole) which is close to that describing the diffusion of Cu in Al ($\simeq$ 138 kJ/mole).

Viscous glide creep may arise from the operation of five viscous drag processes[4] which are related to (a) the segregation of solute atoms to moving dislocations[35] (the Cottrell-Jaswon interaction), (b) the destruction of short range order[36] (the Fisher interaction), (c) the chemical interaction of solute atoms with extended dislocations[37] (the Suzuki interaction), (d) the stress-induced local ordering of solute atoms[38] (Snoek ordering), and (e) the antiphase boundary interaction[4] in ordered alloys. Most recently, it was shown that for a hypothetical alloy in which the above five viscous drag processes are active, the total creep rate may be given by[39]

$$\dot{\gamma}_g = \frac{4}{A_{C\text{-}J} + A_F + A_S + A_{Sn} + A_{APB}} G \left(\frac{\tau}{G}\right)^3 \qquad [4]$$

where A is an interaction parameter which characterizes the particular viscous drag process operating on the dislocations during glide, and the subscripts C-J, F, S, Sn, and APB refer to the Cottrell-Jaswon interaction,[35] the Fisher interaction,[36] the Suzuki interaction,[37] the Snoek interaction,[38] and the antiphase boundary (APB) interaction, respectively. The expressions of A for the five drag processes were developed and are given elsewhere.[39] The development[39] of Eq. [4] is based on the assumption that the viscous-drag processes arising from the five solute atom-dislocation interactions act sequentially; in the limit, the drag process having the largest value of A dominates the creep behavior (the slowest process).

For the Al-3 pct Cu solid-solution alloy, $A_{APB} = 0$, and calculations reported elsewhere[39] show that the major force retarding the glide of dislocations in dilute Al-Cu alloys arises from the Cottrell-Jaswon interaction,[35] *i.e.*, $A_{C\text{-}J} >> A_F + A_S + A_{Sn}$. Under these conditions, Eq. [4] reduces to

$$\dot{\gamma}_g = \frac{4}{A_{C\text{-}J}} G(\tau/G)^3 \qquad [5a]$$

with

$$A_{C\text{-}J} = \frac{e^2 c b^5 G^2}{kTD_g} \qquad [5b]$$

where e is the atom misfit parameter, c is the solute concentration, and D_g is the diffusion coefficient for the glide process. Substituting the value of $A_{C\text{-}J}$ into Eq. [5a] and rearranging leads to the following normalized expression:

$$\frac{\dot{\gamma} kT}{D_g Gb} = 4\left(\frac{kT}{eGb^3}\right)^2 \frac{1}{c}(\tau/G)^3 \qquad [6]$$

In Figure 7, the normalized creep rates obtained in region II are plotted against the normalized shear stress according to Eq. [3]; D_0 and Q were taken as 0.647 cm^2/s[40] and 151 kJ/mole, respectively. For the purpose of comparison, the normalized creep rates predicted from Eq. [6] are also included in the figure and are represented by three lines which correspond to the three testing temperatures. The presence of a single line for each test temperature reflects the fact that at constant normalized stress, the normalized creep rates predicted for viscous glide from Eq. [6] depend on temperature; $\dot{\gamma} kT/DGb \propto T^2/G^2$. As shown by Figure 7, the normalized experimental data exhibit, despite some experimental scatter, a trend similar to that predicted; the experimental data fall within a narrow band whose upper and lower boundaries correspond to the highest and lowest temperatures,* respectively. Although the stress exponent measured experimentally in region II ($n \simeq 3.2$) is slightly larger than the theoretically predicted value of 3 (Eq. [6]), the agreement between the experimental creep rates and the predicted creep rates, as shown by Figure 7, are within a factor of 2. The very small difference in the value of the stress exponent between theory and experiment may be the result of (a) small contributions from other concurrently active creep processes, especially dislocation climb, to viscous glide and/or (b) the presence of an internal stress[41] during viscous glide in solid solution alloys.

*By contrast, the normalized creep data obtained in region I (Figure 6) scatter about a single straight line.

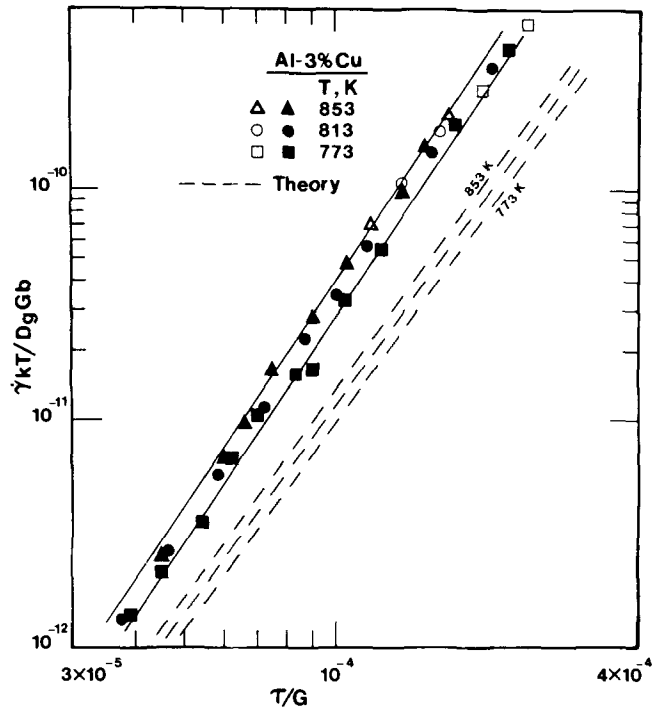

Fig. 7—Normalized creep rate *vs* normalized shear stress (logarithmic scale) for Al-3 wt pct Cu in region II.

C. *The Transition from Region I to Region II*

Recently, a deformation criterion[6,39] which accounts for the creep behavior of a particular solid-solution alloy, whether climb-controlled behavior or glide-controlled behavior, was developed. In addition, the criterion predicts that the two limiting stress exponents of 5 and 3 may be observed in a single alloy at low and intermediate stresses, respectively, provided that the following condition[39] is satisfied:

$$\frac{kT}{D_g b \Sigma A} = B\left(\frac{\Gamma}{Gb}\right)^3 \frac{D_c}{D_g}\left(\frac{\tau}{G}\right)_t^2 \qquad [7]$$

where ΣA is the sum of the values of the interaction parameters for various concurrently active viscous drag processes, B is a dimensionless constant, D_c is the diffusion coefficient for the climb process, and $(\tau/G)_t$ is the normalized transition stress. Under the condition that the force acting on dislocations during glide arises mainly from the Cottrell-Jaswon interaction, Eq. [7] can be written in the following form:

$$\left(\frac{kT}{ec^{1/2}Gb^3}\right)^2 = B\left(\frac{\Gamma}{Gb}\right)^3\left(\frac{D_c}{D_g}\right)\left(\frac{\tau}{G}\right)_t^2 \qquad [8]$$

In Figure 8, Eq. [8] is depicted graphically by plotting $(kT/ec^{1/2}Gb^3)^2$ *vs* $(\Gamma/Gb)^3(D_c/D_g)(\tau/G)^2$ on a logarithmic scale. On this form of plot, Eq. [8] is represented by a solid line at 45 deg; the position of the line was determined previously using the creep data of Al-3 pct Mg.[6]

To provide a direct comparison between the prediction of Eq. [8] and experimental results, the stress range covering both region I and region II along with the transition point for each testing temperature was superimposed on Figure 8 using the following values:

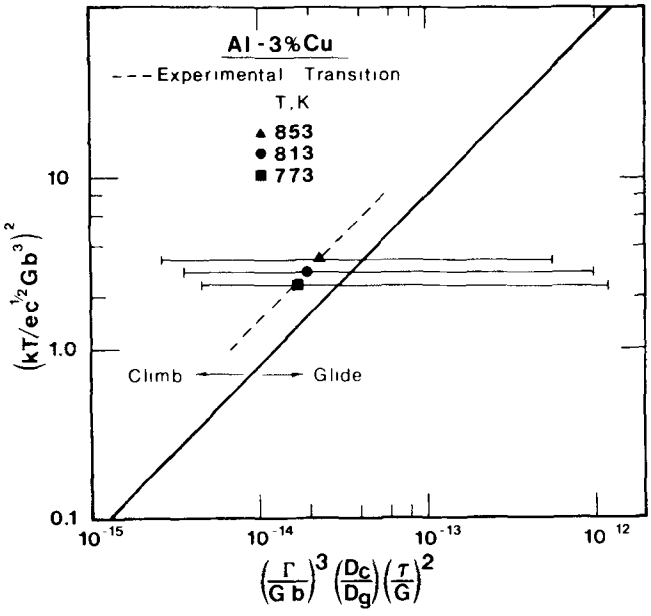

Fig. 8—The glide-climb criterion represented by logarithmically plotting $[kT/ec^{1/2}Gb^3]^2$ *vs* $(\Gamma/Gb)^3\, Dc/Dg\, (\tau/G)^2$. The position of the boundary at 45 deg is determined from the data on Al-3 pct Mg.[5,10] Experimental transition points between regions I and II (taken from Fig. 1), along with horizontal lines representing the square of the stress ranges used in covering these two regions, are shown for Al-3 wt pct Cu at three different temperatures.

$e = 0.142$[42]
$c = 0.013$
$\Gamma = 180$ mJ/m^2 (present investigation)
$D_c = 1.86 \exp(-155/RT)$
and
$D_g = 0.647 \exp(-151/RT)$

The experimental transition points as plotted in Figure 8 not only describe a trend that is consistent with the direction of the boundary between the two types of creep behavior but also are in good agreement with its position; the separation is only a factor of 2.

Present calculations indicate that D_c/D_g is essentially constant over the temperature range used in the investigation; the ratio between D_c/D_g at 853 K and that at 773 K is 1.05. Also, several arguments, reported elsewhere,[22,28] are suggestive of the insensitivity of Γ/Gb to temperature variation. Consideration of the equation representing the deformation criterion of solid-solution alloys (Eq. [8]) along with the information regarding lack of dependence of both D_c/D_g and Γ/Gb on temperature leads to the following prediction: the normalized transition stress between region I (climb) and region II (glide) would decrease with decreasing test temperature from 853 K to 773 K. Experimental results, as shown in Figure 1 and described in Section III–A, are in conformity with this prediction.*

*According to Eq. [8], a decrease in temperature from 853 K to 773 K would result in a decrease in $(D_c/D_g)(\tau/G)^2$ by a factor of 1.4, which cannot be solely accounted for by the very small decrease in D_c/D_g with decreasing temperature.

D. *Region III*

The experimental results in this region, which prevail at high stresses, show three characteristics: (a) the stress exponent is higher than that of region II but is close to that of region I; at 773 K, where region III covers almost two orders of magnitude of creep rate, $n \simeq 4.5$, (b) the creep curve exhibits an extensive primary stage, and (c) the activation energy is considerably higher than those representing self diffusion in Al (144 kJ/mole) and diffusion of Cu in Al (138 kJ/mole).

The above three characteristics, especially that regarding the activation energy for creep, resemble those reported for Al-21 pct Zn under similar experimental conditions; the activation energy reported for Al-21 wt pct Zn at high stresses ($\simeq$ 165 kJ/mole) is higher than those estimated for diffusion of Al and Zn in the alloy (115 and 122 kJ/mole, respectively).

The creep behavior of Al-3 pct Cu in region III, as manifested by the above three characteristics, is not entirely consistent with any of the deformation processes suggested recently to explain the creep behavior of metals and solid-solution alloys at high stresses. First, while the value of the stress exponent and the nature of the creep curve in region III are compatible with some form of dislocation climb process controlled by lattice diffusion,[11,43] the high value of the activation energy for creep (higher than that for lattice diffusion) appears to preclude the operation of such a process. Second, the value of the stress exponent in region III can be explained in terms of a viscous drag process[44] in which the stress dependence of dislocation density is stronger than that reported for solid-solution alloys at intermediate stresses (dislocation density $\alpha \tau^2$), but the presence of extensive primary in the creep curve and the observation of high activation energy are not expected under the condition of viscous glide control. Finally, the high value of the activation energy for creep in region III tends to rule out the possibility of the operation of any deformation process that is controlled by pipe diffusion[45] (whether climb or viscous glide).

It is clear from the preceding discussion that the creep behavior at high stresses is controlled by an unknown process and that more work is needed to identify the origin of this process.

E. *The Transition from Region II to Region III*

The transition in the creep behavior of Al-3 pct Cu from region II ($n \simeq 3.2$) to region III ($n > 3.2$) was reported for a number of alloys, whose creep behavior at intermediate stresses, like that of the present alloy, exhibit the characteristics of viscous glide. Earlier analyses[12,46] of the creep data of those alloys suggested that excellent agreement exists between the experimental values of the transition stresses and those of critical stresses required for the breakaway of dislocations from solute-atom atmospheres; the critical normalized stress as a function of temperature is given by[46]

$$\tau/G = 0.05\, ce^2Gb^3/kT \qquad [9]$$

The consistency between the prediction of Eq. [9] and the present experimental data is demonstrated by two points: (a) the values of the normalized experimental transition stresses, when plotted against ce^2Gb^3/kT on a logarithmic scale in Figure 9, fall very close to the solid line representing Eq. [9]; for the purpose of comparison, data on other solid-solution alloys are also included in the figure, and (b) according to Figure 1, the normalized experimental transition stress between region II and region III increases with decreasing temperature (Section III–A), a finding which is predicted by Eq. [9] ($\tau/G \alpha G/T$). In addition, the prediction of Eq. [9] ($(\tau/G)_{II-III} \alpha G/T$) along with the implication of Eq. [8] ($(\tau/G)_{I-II} \alpha T^2/G^2$) accounts for the observation made in Section III–A that region II (viscous-glide control) covers an increasing range of measurable shear strain rates (or stresses) with decreasing temperature.

The good agreement between the prediction of Eq. [9] and experimental data regarding the transition from region II to region III provides additional evidence that

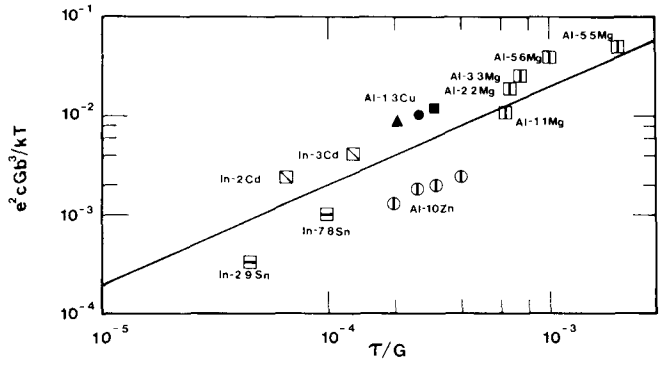

Fig. 9—Correlation between the condition of the breakaway of dislocations from solute-atom atmospheres (Eq. [9]) and experimental data of solid-solution alloys including Al-3 wt pct Cu (1.3 at. pct Cu). The compositions of the alloys are given in atomic percent.

region III (high-stress region) is not controlled by any form of viscous glide process.

F. *Ductility as a Function of Strain Rate*

Ductility, defined as the percentage of elongation to fracture, is a sensitive function of the stress exponent for creep. The dependence of ductility on the stress exponent may be expressed in this form[15]

$$e \text{ pct} = \left[\exp \frac{c}{n} - 1\right] \times 100 \qquad [10]$$

where $c = \ln 400/n$.

The data of Figure 1 show that at 853 K, the stress exponent increases from a value of 4.5 at low stresses (low-strain rates), to a value of 3.2 at intermediate stresses (intermediate strain rates), and then increases again. By contrast, the stress exponent reported for Al under similar experimental conditions exhibits a constant value of about 4.5 over the same range of stresses except at high stresses where it increases as a result of the breakdown of the creep power law.

Applying Eq. [10] to the above experimental findings on Al-3 pct Cu and Al leads to the following expectations: (a) the ductility of Al-3 pct Cu will exhibit a maximum over an intermediate strain rate range where the stress exponent is 3.2, (b) the value of this maximum will be equal to 350 pct, and (c) no variation in the ductility of Al will occur over the whole range of strain rates except at the very high rates where ductility will begin to decrease. While the elongation data of Al exhibit a trend which is in agreement with expectation (c), the data of Al-3 pct Cu show the presence of two peaks and not a single peak as expected. These two peaks occur at tensile strain rates of 10^{-4} s^{-1} and 6×10^{-4} s^{-1}, respectively.

Of these two peaks in the ductility curve of Al-3 pct Cu, the one at $\dot{\varepsilon} = 10^{-4}$ s^{-1} (equivalent to $\dot{\gamma} = 1.5 \times 10^{-4}$ s^{-1}) appears most likely to reflect the variation in the stress exponent for creep in the alloy for three reasons. First, the peak occurs at a strain rate which is slightly lower than that representing the center of region II ($n \simeq 3.2$). The small difference in position between the peak in ductility and the center of region II may be attributed, in part, to the fact that strain rates of Figure 1 (creep data) represent steady-state rates while those of Figure 5 (ductility data) correspond to initial rates.* Second, the magnitude of the peak ($\simeq$ 355 pct) is in excellent agreement with the prediction of Eq. [10] ($\simeq$ 350 pct) when the value of the stress exponent in region II is used ($n = 3.2$). Third, the second peak occurring at $\dot{\varepsilon} = 6 \times 10^{-4}$ s^{-1} (equivalent to $\dot{\gamma} = 9 \times 10^{-4}$ s^{-1}) is very narrow and cannot, therefore, be associated with region II which extends over two orders of magnitude of strain-rate.

*It is worth mentioning that a neck, once developed, will deform at a strain rate which is effectively higher than the remainder of the gage length.

The similarity in value between the two stress exponents for creep in region I and region III and the absence of significant cavitation in deformed specimens should result in a symmetrical ductility curve about the center of region II. However, as seen in Figure 5, the values of ductility at strain rates higher than that representing the peak fall rapidly, resulting in an unsymmetrical ductility curve. A possible reason which may explain such a trend and which may account for the presence of the second peak is now offered.

Consideration of the details of the interaction between solute atoms and moving dislocations suggests the presence of three domains of behavior, depending on the value of the strain rate. In the first domain, strain rates are lower than the transition strain rate between region II and region III, and solute atoms can diffuse sufficiently rapidly that they are able to form atmospheres around the slowly moving dislocations. This condition produces viscous glide creep. In the third domain, strain rates are higher than the transition strain rate and dislocations break away from solute atom atmospheres. Under this condition, the creep behavior is not controlled by viscous glide but by an unknown process having an activation energy higher than that for lattice diffusion. In the second domain, strain rates approach the value of the transition strain rate, and dislocations in some regions of the specimen may, due in part to the presence of high stress concentration points which raise the applied stress, break away from their solute atmospheres. Once breakaway in these regions occurs, dislocations are accelerated to higher velocities. However, when these fast dislocations are restrained by internal stress fields of other dislocations or obstacles, the solute-atom atmosphere forms again, and the dislocation reverts to the slow velocity. Hence in this region where $\dot{\gamma} \rightarrow \dot{\gamma}_t$, velocity transitions occur repeatedly, creating a situation which is essentially identical to that responsible for serrated flow in alloys and which can lead to a loss in ductility; as reported elsewhere,[47] the occurrence of serrated flow in materials is accompanied by a corresponding decrease in ductility. When this predicted loss in ductility is subtracted from the values of elongation to fracture in a hypothetical ductility curve (Figure 10), the result is a ductility curve that resembles the experimental ductility plot (Figure 5) in two ways: the presence of a sharp drop in ductility at strain rates slightly higher than that representing the peak, and the occurrence of the second peak.

According to the above argument, the presence of a second peak in the ductility curve of a solid-solution alloy is a consequence of a drop in ductility values at strain rates

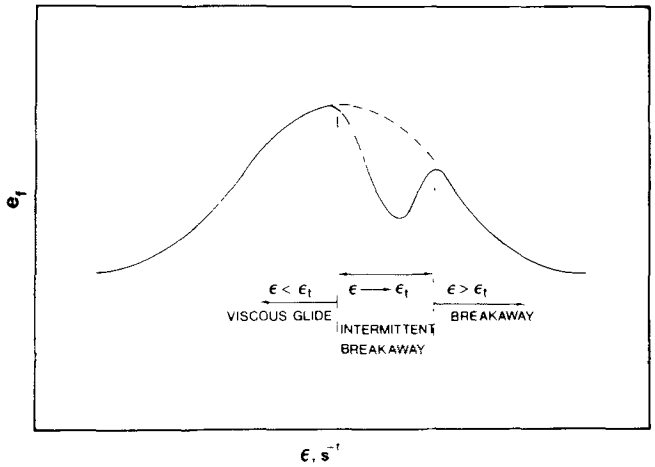

Fig. 10—Schematic ductility curve for a hypothetical solid-solution alloy, showing the region of a rapid drop in the expected ductility as a result of intermittent breakaway of dislocations from a series of consecutive solute atmospheres.

that are approaching the transition strain rate between region II and region III. Because this drop in ductility is expected to occur over a very narrow range of strain rates, it is quite possible that such a peak may not be observed, or may be masked, under the following conditions: (a) the deformation region controlled by viscous-glide creep (region II) is very small, and/or (b) ductility data are obtained on an Instron machine by using widely-spaced values of strain rates in the domain preceding the transition strain rate between region II and region III.

V. CONCLUSIONS

1. The creep behavior of Al-3 pct Cu, when studied in the solid-solution range, divides into three regions: low-stress region (region I), intermediate-stress region (region II), and high-stress region (region III).
2. In regions I and II, the creep characteristics including the stress exponent, the shape of the creep curve, the activation energy for creep, and the values of normalized creep rates are consistent with dislocation climb and viscous glide, respectively. Also, the experimental transition stresses between region I and region II agree with those predicted from the deformation criterion for solid-solution alloys.
3. The normalized creep data of Al-3 pct Cu in region I, when combined with the well-established cubic dependence of the normalized creep rate on the normalized stacking fault energy, Γ/Gb, results in a value of $\Gamma = 180$ mJ/m^2.
4. In region III, the high value of the activation energy measured 205 kJ/mole rules out the possibility of the operation of some form of dislocation climb controlled by lattice diffusion. In addition, the close correspondence between the advent of region III and dislocation breakaway from a solute-atom atmosphere, together with the observation of high activation energy and extensive primary creep in region III, are not compatible with viscous glide controlled by either lattice or core diffusion.
5. Two peaks are present in the ductility curve of Al-3 pct Cu. The first peak occurs at an initial strain rate of 1×10^{-4} s^{-1} and reflects the variation of the stress exponent for creep in the alloy with strain rate. The second peak occurs at an initial strain rate of 6×10^{-4} s^{-1} and may arise from a sharp drop in ductility produced by solute drag under the condition of intermittent breakaway of dislocations from a series of consecutive solute atmospheres; this condition prevails over a very narrow domain at strain rates approaching the transition strain between region II and region III.

ACKNOWLEDGMENTS

This work was supported by the National Science Foundation under Grant No. DMR 8420615. Thanks are extended to Janice Johnson for typing the manuscript.

REFERENCES

1. O. D. Sherby and P. M. Burke: *Prog. Mater. Sci.*, 1968, vol. 13, pp. 325-90.
2. J. E. Bird, A. K. Mukherjee, and J. E. Dorn: *Quantitative Relation Between Properties and Microstructures*, D. G. Brandon and A. Rosen, eds., Israel Universities Press, Jerusalem, 1969, pp. 255-342.
3. W. R. Cannon and O. D. Sherby: *Metall. Trans* , 1970, vol. 1, pp. 1030-32.
4. J. Weertman: *Trans. Amer. Inst. Mining Eng.*, 1960, vol. 218, pp. 207-18.
5. F. A. Mohamed and T. G. Langdon: *Acta Metall.*, 1974, vol. 22, pp. 779-88.
6. K. L. Murty, F. A. Mohamed, and J. E. Dorn: *Acta Metall.*, 1972, vol. 20, pp. 1009-18.
7. F. A. Mohamed and T. G. Langdon: *Metall. Trans. A*, 1975, vol. 6A, pp 927-28.
8. F. A. Mohamed: *Metall. Trans. A*, 1978, vol. 9A, pp. 1013-15.
9. P. Yavari, F. A. Mohamed, and T. G. Langdon: *Acta Metall.*, 1981, vol. 29, pp. 1495-1507.
10. M. S. Soliman and F. A. Mohamed: *Mater. Sci. Eng.*, 1982, vol. 55, pp. 111-19.
11. P. Yavari and T.G. Langdon: *Acta Metall.*, 1982, vol 30, pp 2181-96.
12. M. S. Soliman and F. A. Mohamed: *Metall. Trans. A*, 1984, vol. 15A, pp. 1893-1904
13. M. A. Burke and N. D. Nix: *Acta Metall.*, 1975, vol. 23, pp. 793-98.
14. A. K. Ghosh and R. A. Ayres: *Metall. Trans. A*, 1976, vol. 7A, pp. 1589-91.
15. F. A. Mohamed: *Scripta Metall.*, 1979, vol. 13, pp. 87-90
16. F. A. Nichols: *Acta Metall.*, 1980, vol. 27, pp. 663-73.
17. I. H. Lin, J. P. Hirth, and E. W. Hart: *Acta Metall.*, 1981, vol. 29, pp. 819-27.
18. M. S. Mostafa and F. A. Mohamed. *Metall. Trans. A*, 1986, vol. 17A, pp. 365-66.
19. F. A. Mohamed, K. L. Murty, and J W. Morris, Jr : *Metall. Trans.*, 1973, vol. 4, pp 935-40
20. H. Ishikawa, F. A Mohamed, and T. G. Langdon. *Phil. Mag.*, 1975, vol. 32, pp. 1269-71.
21. F. A Mohamed, M. M. I Ahmed, and T. G Langdon: *Metall. Trans. A*, 1977, vol. 8A, pp. 933-38
22. B S. Chin, W. D. Nix, and G M Pound: *Metall. Trans A*, 1977, vol. 8A, pp. 1523-30.
23. H I. Huang, O. D Sherby, and J. E. Dorn: *Trans. AIME*, 1956, vol. 206, pp. 1385-88.
24. A. K. Mukherjee, J. E. Bird, and J E. Dorn: *Trans. ASM*, 1969, vol. 62, pp. 155-79.
25. J. Weertman: *J. Appl Phys.*, 1955, vol. 26, pp. 1213-17.
26. J. Weertman *J Mech. Phys. Solids*, 1956, vol. 4, pp. 230-34.
27. I. S. Servi and N. J Grant: *Trans. AIME*, 1951, vol. 191, pp. 909-16.
28. P C. Gallagher. *Metall. Trans* , 1970, vol 1, pp. 2429-61
29. F. A Mohamed and T. G Langdon: *J. Appl. Phys.*, 1974, vol. 45, pp. 1965-67.
30. A S. Argon and W. C. Moffatt: *Acta Metall.*, 1981, vol 29, pp. 293-99.
31. A S. Argon and S Takeuchi: *Acta Metall* , 1981, vol. 29, pp. 1877-84.
32. V. C Kannan and G Thomas: *J. Appl Phys.*, 1966, vol. 37, pp. 2363-70.
33 A. Goel, T. J. Ginter, and F. A. Mohamed: *Metall. Trans. A*, 1983, vol. 14A, pp. 2309-18.
34. J Weertman: *J. Appl. Phys.*, 1957, vol 28, pp. 1185-89.
35. A. H Cottrell and M. A Jaswon. *Proc. R. Soc London, Ser. A*, 1949, vol. 199, pp 104-14.
36. J. C. Fisher: *Acta Metall.*, 1954, vol. 2, pp 9-10.
37. H. Suzuki: *Sci. Rep. Research Inst. Tohoku Univ.*, 1952, vol. A4, pp 455-63.
38 J. Snoek: *Physica*, 1942, vol. 9, pp. 862-64
39. F. A. Mohamed: *Mater. Sci. Eng.*, 1983, vol. 61, pp. 149-65.
40. N. L. Peterson and S. J. Rothman: *Phys. Rev.*, 1970, vol. B1, pp 3264-73.

41. S. H. Hong and J Weertman: *Acta Metall.*, 1986, vol. 34, pp. 743-51.
42. H. W. King: *J. Mater. Sci.*, 1966, vol. 1, pp 79-90
43 K L. Murty: *Scripta Metall* , 1973, vol. 7, pp. 899-904.
44. H. Oikawa, K Sugawara, and S Karashima. *Trans. Jap. Inst. Metals*, 1978, vol. 19, pp. 611-16.
45. S. L. Robinson and O D. Sherby. *Acta Metall.*, 1969, vol. 17, pp 109-25.
46 F. A Mohamed. *Mater. Sci Eng* , 1979, vol 38, pp. 73-80
47. A S Keh, Y Nakada, and W. C. Leslie. Dislocation Dynamics, A. R. Rosenfield, G T Hahn, A. L Bement, Jr , and R. I. Jaffee, eds , McGraw-Hill, New York, NY, 1968, pp 381-408.